

Giant low surface brightness halos in distant radio galaxies: USS0828+193

M. Villar-Martín¹, J. Vernet², S. di Serego Alighieri², R. Fosbury³, L. Pentericci⁴,
M. Cohen⁵, R. Goodrich⁶, A. Humphrey¹

¹*Dept. of Physical Sciences, University of Hertfordshire, College Lane, Hatfield, Herts, AL10 9AB, UK*

²*Osservatorio Astrofisico di Arcetri, Largo E. Fermi 5, I-50125, Firenze, Italy*

³*Space Telescope European Coordinating Facility, Karl Schwarzschild Str. 2, D-85748 Garching, bei Muenchen, Germany*

⁴*Max Planck Institute fur Astronomie, Konigstuhl 17, D-69117 Heidelberg, Germany*

⁵*California Institute of Technology, Mail Stop 105-24, Pasadena, CA 91125, USA*

⁶*W.M. Keck Observatory 65-1120 Mamalahoa Highway, Kamuela, HI 96742, USA*

ABSTRACT

We present results on the spectroscopic study of the ionized gas in the high redshift radio galaxy USS0828+193 at $z=2.57$. Thanks to the high S/N of the emission lines in the Keck spectrum, we have been able to perform a detailed kinematic study by means of the spectral decomposition of the emission line profiles. This study reveals the existence of two types of material in this object: a) a low surface brightness component with apparent quiescent kinematics consistent with gravitational motions and b) a perturbed component with rather extreme kinematics. The quiescent halo extends across the entire object for ~ 80 kpc. It is enriched with heavy elements and apparently ionized by the continuum from the active nucleus.

The properties of the quiescent halo and its origin are discussed in this paper. We propose that it could be part of a structure that surrounds the entire object, although its nature is not clear (a rotating disc? low surface brightness satellites? a cooling flow nebula? material ejected in galactic winds? other?).

Key words: galaxies: individual: USS 0828+193 – galaxies: formation – galaxies: active – cosmology: early Universe

1 INTRODUCTION

Extended Ly α regions are a common feature of high redshift radio galaxies ($z > 2$, HzRG) and quasars (Heckman et al. 1991; see also narrow band Ly α images of HzRG in, e.g. Kurk et al. 2001; Chambers, Miley & van Breugel 1990; McCarthy et al. 1990b). Most morphological and kinematic studies are based on the high surface brightness regions. These regions are clumpy, irregular and often aligned with the radio axis. They are characterized by extreme kinematics, with measured FWHM and velocity shifts ≥ 1000 km s⁻¹ (Baum & McCarthy 2000, Villar-Martín, Binette & Fosbury 1999, McCarthy, Baum & Spinrad 1996), compared to values of \sim few hundreds in low redshift radio galaxies (Baum, Heckman & van Breugel 1990, Tadhunter, Fosbury & Quinn 1989). Although gravitational motions cannot be rejected, it is likely that a perturbing mechanism is responsible for the extreme kinematics. The apparent connection between the radio and the kinematic properties suggests that such a mechanism could be shocks generated by the interac-

tion between the radio outflow and the gas in situ (van Ojik et al. 1997). Galactic winds (Heckman, Armus & Miley 1990) are an alternative possibility.

In addition to these regions, low surface brightness Ly α halos extending beyond the radio structures have been detected in some HzRG. The kinematic properties of such halos have been studied in detail only in one case, the radio galaxy MRC1243+036 (van Ojik et al. 1996). The halo shows quiescent kinematics [FWHM(Ly α) ~ 250 km s⁻¹] compared to the regions inside the radio structures [FWHM(Ly α) ~ 1200 km s⁻¹]. The authors propose that the halo is a large rotating gaseous disc originating from the accretion associated with the formation of the galaxy.

Such quiescent low surface brightness halos (LSBHs, hereafter) are important since they show the gas properties unaffected by kinematic perturbations. We are undertaking a research program using high S/N Keck spectroscopy of a sample of high redshift radio galaxies ($z \geq 2.5$) whose goal is to search for kinematically unperturbed Ly α halos in HzRG.

We will study the kinematic and ionization properties, as well as observed properties such as surface brightness, size and luminosity. Constraints will also be set on the halo mass and its possible origin.

The results on the radio galaxy USS0828+193 are presented in this paper. In a forthcoming paper we will discuss the results on the rest of the sample.

2 OBSERVATIONS AND DATA ANALYSIS

USS0828+193 (Röttgering, Miley & Chambers 1995) ($z=2.57$) is a large radio source (~ 70 kpc)^{*} showing a double morphology and a jet extending from the core to the northern hot spot. The optical HST image shows an irregular morphology consisting of several clumps aligned with the radio axis (Pentericci et al. 1999, see also Fig. 1 top panel in this paper). The high polarization level (~ 10 per cent) implies that the UV rest frame continuum is dominated by continuum from the active nucleus (AGN) scattered by (most probably) dust in the extended gas (Vernet et al. 2001).

The spectra were obtained with the Low Resolution Imaging Spectrometer (LRIS, Oke et al. 1995) with its polarimeter (Goodrich, Cohen, Putney 1995) at the Keck II 10 m telescope in December 1997. We used a 300 line mm^{-1} grating and 1 arcsec wide slit which provide a dispersion of $2.4 \text{ \AA pixel}^{-1}$ and an effective resolution of $\text{FWHM} \sim 10.5 \text{ \AA}$ (instrumental profile). The exposure time was 5 hours. The seeing (~ 1.0 arcsec) was measured with the M5V type star located inside the slit. The slit was oriented along the radio axis, with PA 44° (Carilli et al. 1997). For a more detailed description of the observations and data reduction see Vernet et al. 2001.

Each individual frame was calibrated in wavelength and corrected for slit curvature using arc spectra. This initial wavelength calibration was refined using strong sky lines. In order to compensate for residual distortions (shifts) due to flexures in LRIS, we extracted from every frame a section around $\text{Ly}\alpha + \text{NV } 1240$ and one around $\text{CIV } 1550 + \text{HeII } 1640$ (CIV and HeII respectively, hereafter). The individual subframes corresponding to the same spectral range were spatially aligned (using the continuum centroid) and combined. The two final frames (one for $\text{Ly}\alpha + \text{NV}$ and another one for $\text{CIV} + \text{HeII}$) were also spatially aligned, assuming that the continuum centroid has the same spatial position at all wavelengths. This is reasonable in this small spectral range, taking also into account that the spatial resolution element has a large physical size (~ 5 kpc).

The spectra ($\text{Ly}\alpha + \text{NV}$ and $\text{HeII} + \text{CIV}$ frames) were divided in several apertures along the spatial direction and a spectrum was extracted for each one. The apertures were selected so that the gas has apparently similar kinematic properties across the spatial extension of a given aperture. The apertures were also selected to obtain enough S/N ratio in $\text{Ly}\alpha$, CIV and HeII (if possible) to fit the line profiles (see Figs. 3 and 4). Separate apertures were defined for the gas beyond the radio structures.

^{*} We assume $H_0 = 72 \text{ km s}^{-1} \text{ Mpc}^{-1}$ and $q_0 = 0.5$. In this cosmology, 1 arcsec corresponds to ~ 5 kpc

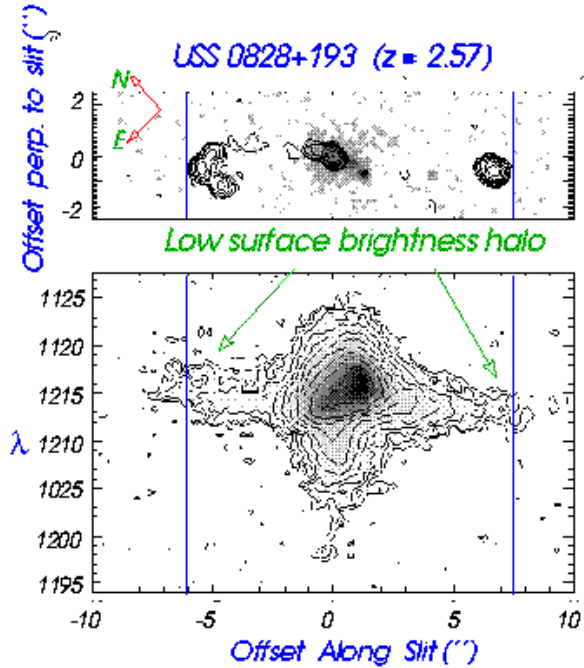


Figure 1. Top: overlay between the optical HST image and the radio VLA contours. The 2-dimensional spectrum of the $\text{Ly}\alpha$ emission line (bottom panel) is spatially aligned with the radio/optical images. The spatial zero is the position of the continuum centroid measured on the Keck spectra. The vertical lines indicate the outer edges of the radio lobe.

3 RESULTS

3.1 Radio/Optical overlay

Figure 1 (top panel) shows the overlay between the optical WFPC2 HST image and VLA contours (see Pentericci et al. 1999 for a description). The 2-dimensional $\text{Ly}\alpha$ Keck spectrum is shown on the bottom panel spatially aligned with the image. We identified the radio core with the brightest component in the NICMOS HST image. Our main conclusions would not be affected if we chose to identify the radio core with the vertex of the ionization cone described by Pentericci et al. (1999) or the brightest optical component.

An interesting feature is already obvious in this figure: a low surface brightness $\text{Ly}\alpha$ halo extending for ~ 16 arcsec or 80 kpc inside and beyond the radio structures. It extends to much larger distances than the material observed on the HST images (~ 4 arcsec). The HST image shows, therefore, only a small fraction of the total distribution of material. The kinematics of this halo is more quiescent than the kinematics of the brightest regions.

3.2 The gas kinematics

We show in Fig. 2 the 2-dimensional spectrum (contours) of the main emission lines. Seven apertures were selected in the spatial direction for the kinematic analysis, which are indicated in Fig. 3. The corresponding 1-dimensional spectra in the $\text{Ly}\alpha$ and the $\text{CIV} + \text{HeII}$ regions are shown in Fig. 4. Apertures 1, 2, 6, 7 correspond to the low surface bright-

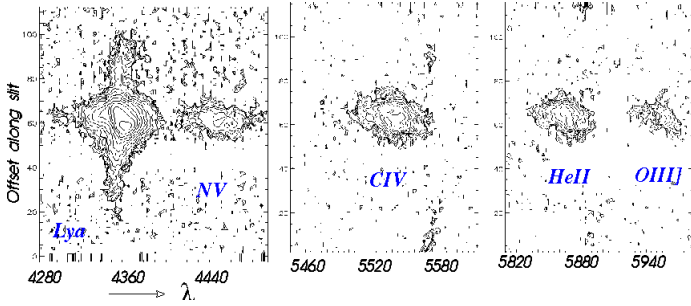


Figure 2. Contour plots of the main emission lines.

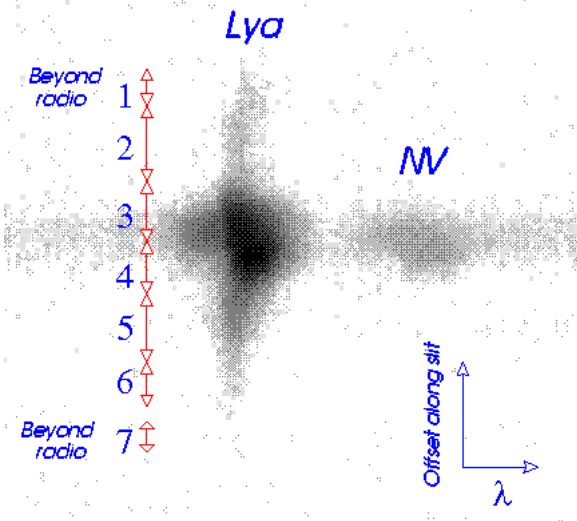


Figure 3. 2-dimensional Ly α +NV spectrum and selected apertures.

ness Ly α halo. Although very noisy, CIV and HeII are detected in apertures 2 and 6 (see Fig. 4).

The Ly α and HeII spectral profiles were analysed and fitted in each aperture with one, two or three Gaussians, depending on the quality of the fit. CIV, in spite of being a strong line, turned out to be very difficult to constrain due to the presence of the doublet components (for a discussion on the uncertainties on interpreting the kinematics of the extended gas in HzRG using rest frame UV emission lines see Villar-Martín et al. 2001). Therefore the results of the multiple component fit are only shown for Ly α and HeII. Those presented for CIV correspond to a single Gaussian fit. For each kinematic component, the FWHM (corrected for instrumental broadening in quadrature) and the velocity shift relative to the emission at the continuum centroid were calculated (the HeII line at the continuum centroid was used to estimate the zero velocity). Some of the fits are shown in Fig. 5.

Three kinematic components are found in Ly α : (i) a narrow component with FWHM $< 400 \text{ km s}^{-1}$ detected in all apertures; (ii) a broad component with FWHM $\sim 1200 \text{ km s}^{-1}$ detected in all apertures except 6 and 7 (note this

is also detected beyond the radio lobe in aperture 1); (iii) a very broad component with FWHM $\sim 2500 \text{ km s}^{-1}$ only found in apertures 3 and 4 (brightest regions). The best fit to the HeII profile reveals two components in apertures 3 and 4 similar (in FWHM) to components (i) and (ii) in Ly α . Narrow HeII (aperture 2) and CIV (apertures 2 and 6) are also detected.

(i) *The narrow component ($< 400 \text{ km s}^{-1}$):* The spatial variation of the kinematic properties of this component are shown on panels *a* (FWHM) and *b* (V_s) in Fig. 6. Different symbols are used for Ly α (circles), HeII (stars) and CIV (triangles). This component extends across the whole object ($\sim 80 \text{ kpc}$) and beyond the radio structures. The kinematic properties are very uniform across the whole spatial extension. There are no obvious changes associated with the radio structures.

Ly α is very sensitive to absorption by neutral hydrogen and the interpretation of the spectral profile in terms of pure kinematics is risky. In fact, van Ojik et al. (1997) found that the entire blue wing of the Ly α (spatially integrated) profile of this galaxy is absorbed by neutral gas associated with the galaxy. However, the fact that a similar narrow component has been found in HeII (which is not a resonance line) strongly supports the existence of a narrow component in Ly α in addition to the broad components. This is also supported by the very narrow profile of CIV and HeII in apertures 2 and 6 and the very narrow peak observed on top of the CIV and HeII lines in the inner apertures, 3 and 4 (see Fig. 4).

(ii) *The broad component ($\sim 1200 \text{ km s}^{-1}$)* (open circles for Ly α , open triangles for CIV and stars for HeII in panels *c* and *d* in Fig. 6). This component is also spatially extended ($\sim 11 \text{ arcsec}$) and with quite uniform FWHM across the object, with no apparent link with the radio structures. This kinematically perturbed gas is also found in the Ly α halo. The measured FWHM is consistent within the errors for the three emission lines (HeII, CIV, Ly α) where it is detected, with marginal evidence for narrower Ly α . This could be due to absorption by neutral hydrogen. This component extends beyond the radio structures (aperture 1). Seeing effects might be responsible for spreading the detection of this component beyond the radio lobes. Astrometry errors are not likely to be responsible (see below).

(iii) *The very broad component ($\sim 2500 \text{ km s}^{-1}$)* (solid circles in panels *c* and *d* in Fig. 6) is spatially extended and it is only detected in Ly α in apertures 3 and 4.

4 DISCUSSION

4.1 The nature of the narrow component

This component (which extends across the entire object and beyond the edge of the radio lobes) shows no apparent association with the radio structures. The kinematic properties are similar to those of low redshift radio galaxies (FWHM and velocity shift of a few hundred km s^{-1} , e.g. Tadhunter, Fosbury & Quinn 1989). This suggests that there is no (or little) interaction and this gas is unperturbed by the jet/radio lobes. Absorption of Ly α photons could explain the difference in the velocity shift of Ly α and HeII in the inner apertures. The kinematics of this narrow component is consistent with gravitational motions.

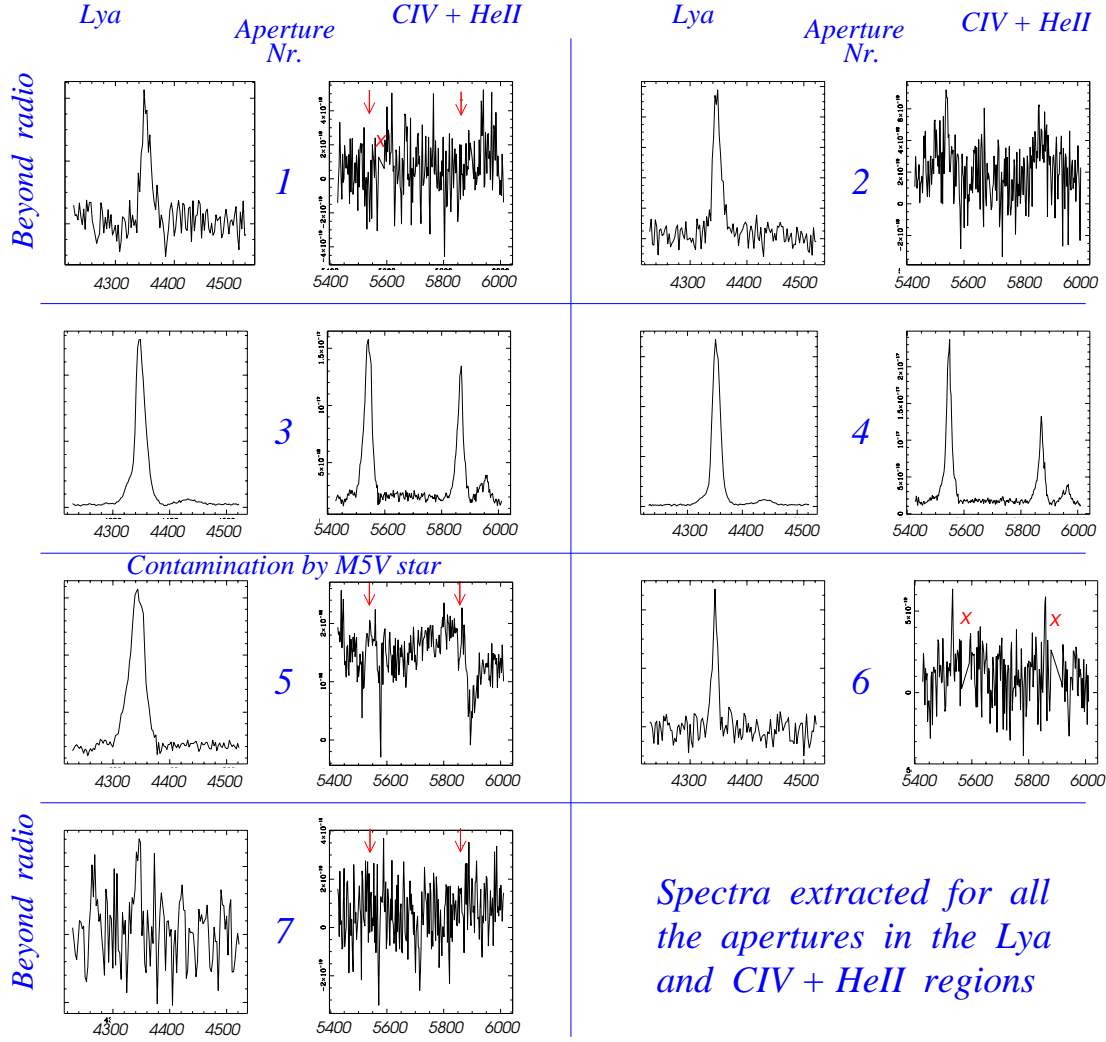


Figure 4. Spectra extracted for the seven apertures indicated in Fig. 3. The expected position for the CIV and HeII lines has been indicated with open arrows in the noisiest spectra. CIV and HeII are detected in the low surface brightness halo (see spectra of apertures 2 and 6). Therefore, the gas is ionized and contains heavy elements. There is marginal evidence for continuum detection in the halo. The interpolation (indicated with 'x') on the red side of CIV and HeII in apertures 1 and 6 was done to remove residuals from sky emission lines.

This gaseous component also emits CIV and HeII lines. It is the first time that lines other than Ly α are detected from the low surface brightness halo of a HzRG. This implies that the gas is ionized. It is not a 'mirror' of neutral hydrogen that reflects Ly α by resonant scattering (Villar-Martín, Binette & Fosbury 1996).

There is marginal evidence for continuum detection in the halo (see Fig. 4). The nature of this continuum is very uncertain. It could be due to scattered light, although stars cannot be rejected. The large equivalent widths of CIV and HeII suggest that the gas is not ionized by stars, but rather by a mechanism related to the active nucleus. This is also implied by the CIV/HeII \sim 1 value measured for the narrow component (at least in aperture 6 and maybe also aperture 2, see Fig 4), similar to the ratio measured in aperture 3 and consistent with measurements in other HzRG

(e.g. Villar-Martín, Tadhunter & Clark 1997). This suggests the same ionization mechanism in the low surface brightness halo and the bright regions, in spite of the different kinematic properties. Since the halo extends beyond the radio structures where shocks are unlikely to be present, the ionization mechanism is probably ionization by the central AGN (ionization by the continuum generated by hot shocked gas is an alternative mechanism).

On the other hand, the detection of CIV emission shows that the halo has been enriched with heavy elements at very large distances from the nuclear region. It is not possible to constrain the metallicity using only the CIV/HeII ratio, but solar abundances are certainly possible (Villar-Martín, Tadhunter & Clark 1997, Vernet et al. 2001). A galactic wind, whose presence is suggested by the broad component

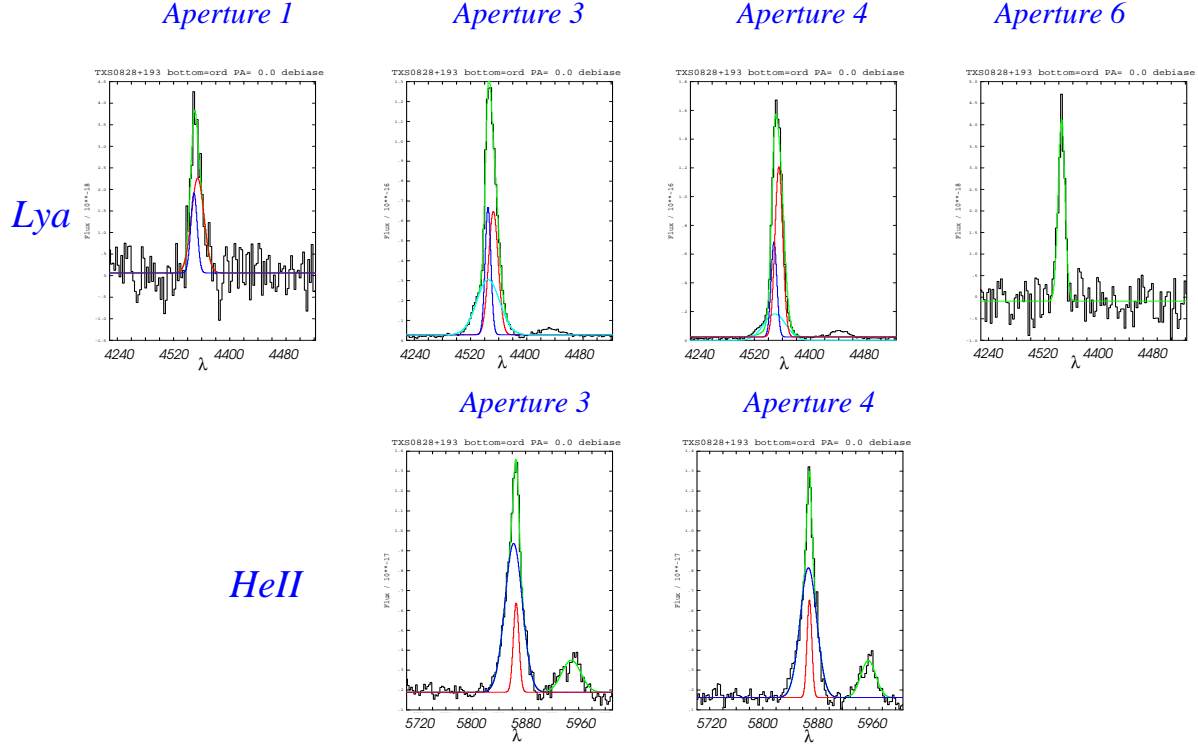


Figure 5. Examples of some of the fits to the $\text{Ly}\alpha$ and HeII lines. The fit and the individual components are shown.

detected at similar distance from the nucleus, might be the mechanism responsible for the enrichment of the gas.

4.2 The nature of the broad (ii) and very broad (iii) components

The broad component ($\sim 1200 \text{ km s}^{-1}$) is apparently detected beyond the Eastern radio lobe. Errors in the Astrometry are unlikely to be responsible: if the active nucleus were located at the vertex of the ionization cone described by Pentericci et al. (1999) or at the brightest optical feature, the broad component would extend even further beyond the edge of the radio lobe. However, we do not discard the possibility that seeing effects might be smearing the emission enough that the broad component actually does not extend beyond the radio lobes.

If the detection beyond the radio structures is real, this implies that the motions of this gas are not a consequence of jet-cloud interactions. Evidence for perturbed gas beyond radio structures has been found in other objects (e.g. Villar-Martín, Binette and Fosbury 1999, Solórzano-Iñarraea, Tadhunter & Axon 2001). Galactic winds could be an alternative possibility. Clouds exposed to ram pressure of the wind can be accelerated to several hundred km s^{-1} and shifted by $\sim 1000 \text{ km s}^{-1}$ (Heckman, Armus & Miley 1990). The integration along the line of sight through several such clouds could explain the broad FWHM of this component. Gas free-falling into the galaxy during the formation process from a large distance can also explain FWHM of this order (Lehnert & Becker 1998). The nature of the very broad component ($\sim 2500 \text{ km s}^{-1}$) in apertures 3 and 4 is not clear. It might

be scattered light from a hidden broad line region (Vernet et al. 2001).

4.3 Mass and density of the ionized gas in USS0828+193

(Hereafter, we will refer to the gas emitting the narrow component as the low surface brightness halo, LSBH).

The integrated $\text{Ly}\alpha$ flux $F_{\text{Ly}\alpha}$ of the LSBH along the slit is $1.64 \times 10^{-15} \text{ erg s}^{-1} \text{ cm}^{-2}$, which corresponds to a luminosity $L_{\text{Ly}\alpha} = 3.8 \times 10^{43} \text{ erg s}^{-1}$. For pure case B recombination and $T = 10^4 \text{ K}$, $L_{\text{Ly}\alpha}$ is given by (McCarthy et al. 1990a):

$$L_{\text{Ly}\alpha} = 4 \times 10^{-24} n_e^2 f V \text{ erg s}^{-1} \quad (1)$$

where f is the volume filling factor of the gas, n_e the electronic density and V is the total volume inside the slit.

We have calculated the volume assuming that the gas of the LSBH is ionized by the active nucleus (see §4.1) and is homogeneously distributed. In this scenario, the ionized halo has a biconical geometry. We have assumed that the cone axis is on the plane of the sky with an opening angle for the individual cones of $\sim 90^\circ$ (Barthel 1989). The 2-dimensional spectra show an extension of $\sim 8 \text{ arcsec}$ (40 kpc) along the slit from the AGN. The volume of the bi-cone slice included in the slit (1 arcsec wide or 5 kpc) is $\sim 3.2 \times 10^{68} \text{ cm}^3$. Assuming $f = 10^{-5}$ (McCarthy et al. 1990a), we obtain $n_e \sim 50 \text{ cm}^{-3}$. This is a very crude estimate. Large uncertainties are due to: a) possible scatter on the f values. Values for f of the order of 10^{-7} - 10^{-8} have been estimated for $\text{Ly}\alpha$ nebulosities associated with high redshift quasars (Heckman

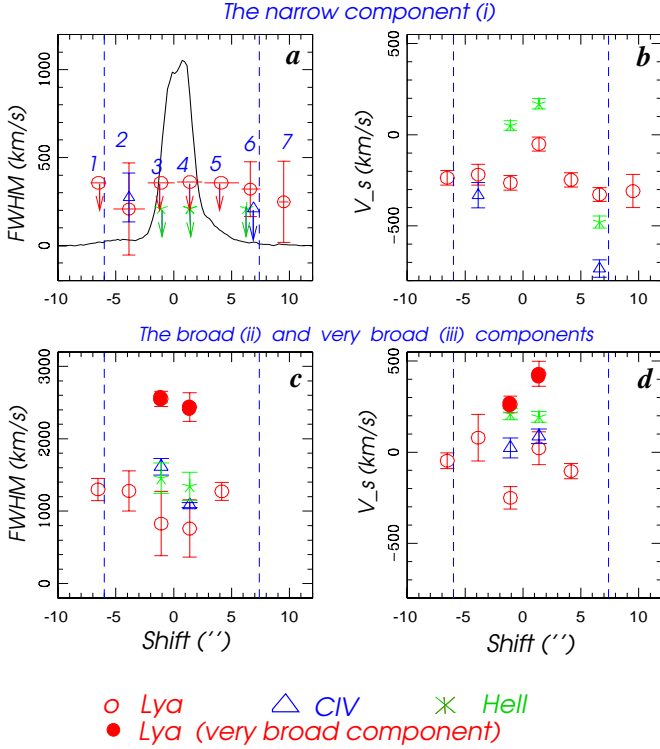


Figure 6. Kinematic properties of the individual components detected in the different apertures. The FWHM appears on the left panels and the velocity shift relative to the HeII emission at the continuum centroid is plotted on the right panels. The narrow component is plotted in panels *a* and *b* and the broad and very broad components are plotted in panels *c* and *d*. The dashed vertical lines mark the outer edge of the radio lobes. Arrows indicate upper limits. The horizontal lines in panel *a* show the spatial extension of the aperture indicated with a number. Notice the uniform properties of the narrow component across the whole object and the similarity with low redshift radio galaxies kinematic properties. The detection of the broad component (panels *c* and *d*) beyond the radio structures is also interesting, since it suggests that jet-cloud interactions are not responsible for the perturbed motions.

et al. 1991) and some low redshift radio galaxies (Clark et al. 1998); b) the fact that the measured Ly α luminosity is probably lower than the case B value (due to the dust and/or neutral hydrogen absorption) and c) the assumptions on the geometry. The estimated n_e value is likely to be a lower limit for the density and it could be at least one order of magnitude higher.

The mass of ionized gas in the LSBH is given by

$$M(H^+) = n_e \times V \times m_p \times f \quad (2)$$

where V is in this case the total volume of ionized gas and m_p the mass of the proton. (We assume that the density is constant across the halo for simplicity, but it is possible that the density increases inwards). Considering the two cones we obtain a total volume of $2.3 \times 10^{69} \text{ cm}^3$ and therefore $M(H^+) \sim 9.6 \times 10^8 M_\odot$, for $n_e = 50 \text{ cm}^{-3}$. This is probably an upper limit. Since $M(H^+) \propto f^{1/2}$ and taking into account the uncertainties on f , the mass could be at least ten times lower.

The halo material outside the ionization cones is likely

to be neutral (or have a low ionization level due to, for instance, metagalactic radiation). Evidence for reservoirs of neutral gas associated with distant radio galaxies has been found by van Ojik et al. (1997). The authors found that the Ly α profile in eleven (including USS0828+193) out of eighteen distant radio galaxies shows deep troughs which they interpret as HI absorption by absorbers that are likely to be physically associated with the galaxy hosting the radio source or its direct environment[†].

The LSBH in USS0828+193 (and other HzRG) could be part of a gaseous reservoir that surrounds the object completely. The gas outside the ionization cones is neutral and we see it in absorption and the gas inside the cones is ionized and we see it in emission. If we assume that the neutral gas of the halo has the same density and filling factor as the ionized fraction, we obtain $M(H^0) \sim 2.4 \times 10^9 M_\odot$. The mass of ionized ($T \sim 10^4 \text{ K}$) and neutral gas in the halo is therefore $M_{H^++H^0} \sim 3.4 \times 10^9 M_\odot$.

Following a similar procedure, we obtain $n_e \sim 150 \text{ cm}^{-3}$ for the broad line emitting gas (the same f and cone opening angle were used). To calculate the volume, two cones of height 4 and 6 arcsec respectively were considered. These are the projected distance values at which the broad component is detected at both sides of the continuum centroid (see Fig. 6). This gives a volume of $\sim 1.3 \times 10^{68} \text{ cm}^3$ inside the slit and $1.2 \times 10^{69} \text{ cm}^3$ as the total volume inside the cones. The mass of broad emission line gas inside the ionization cones is then $\sim 1.5 \times 10^9 M_\odot$.

We conclude that a large fraction of the gaseous (with $T \leq 10^4 \text{ K}$) mass in HzRG might be in large halos that surround the entire object. Part of the halo (the gas inside the ionization cones) is ionized and we see it as low surface brightness line emission. The rest is neutral (or with very low ionization level) and we see it as absorption features imprinted on the Ly α profile

4.4 The origin of the LSBH in USS0828+193

We have considered several scenarios:

- A rotating disc (evidence for large discs associated with low redshift radio galaxies is discussed in §4.5.1). Signs for rotation of the extended gas in nearby radio galaxies have been found by several authors (Heckman et al. 1985, Baum, Heckman & van Breugel 1990, Tadhunter, Fosbury & Quinn 1989). In this case, $M_{rot} = \frac{R V^2}{G \sin i^2}$ where R is the radius of the disc (40 kpc), V is half the amplitude of the rotation curve and i is the inclination angle of the disc with respect to the plane of the sky. This formula is applicable when we measure the rotation along the line of nodes. Velocity curves that resemble rotation have been found in several HzRG, but it is not clear whether this is an effect of multiple kinematic components (Villar-Martín et al. 2001).

The current data do not allow us to set any constraint on

[†] An interesting case is the radio galaxy MRC0943-242 ($z = 2.92$), which shows large scale absorption troughs (Röttgering et al. 1995, Binette et al. 2000), both in Ly α and CIV. Binette et al. concluded that the absorbing gas is metal poor ($Z \sim 0.01 Z_\odot$) and is located much further outside the zone of influence of the radio jet cocoon

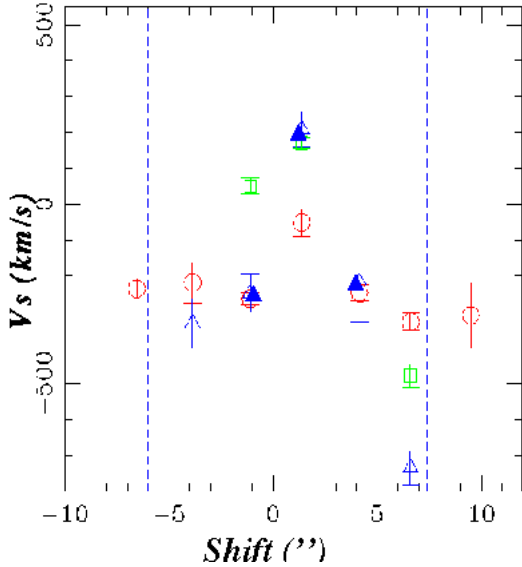


Figure 7. Same as panel *b* in Fig. 6 but with the measured velocity shift for the very narrow peak observed in CIV in the inner apertures (solid triangles). CIV follows a similar pattern to Ly α .

the mass if the halo is a rotating disc: we do not have information on the inclination angle of the disc (imaging would help to constrain it), neither on the direction of the line of nodes, which is likely to be misaligned with respect to the slit position. Van Ojik et al. (1996) propose that the giant Ly α halo associated with the radio galaxy MRC 1243+046 ($z=3.6$) has settled as a rotating disc whose orientation (the plane of the disc) is within $\sim 20^\circ$ of the orientation of the radio axis. However, this is contrary to the trend observed in low redshift powerful radio galaxies with signs of rotation. In such objects, the rotation axis of the gas and the radio axis trend to be aligned within 20° (Heckman et al. 1985). If this is the case for the LSBH in USS0828+193, the rotation axis would be approximately along the slit, since this was aligned with the radio axis.

The Ly α velocity curve of the narrow component in USS0828+193 does not resemble a standard Keplerian rotation curve for a slit located along the line of nodes. However, it is interesting to note that the observed pattern is similar to what we expect from a rotating disc if the slit was not aligned with the line of nodes, but rather close to the perpendicular direction and with some impact parameter with respect to the rotation center (i.e. there is a distance between the center of the slit and the center of rotation). Such a pattern is expected if the disc has a certain inclination relative to the plane of the sky. A close analysis of the CIV line profile in the two inner apertures (3 and 4, see Fig. 4) reveals the presence of a very narrow peak (on top of a dominant broader component). The velocity shift of this narrow peak has been plotted in Fig. 7 (solid triangles); CIV shows a pattern similar to Ly α .

3-dimensional spectroscopy would be very valuable to obtain information about the geometry and the kinematic pattern along different directions across the halo.

- A virialized system: The halo could be a virialized system that consists of N individual clouds of mass m that

move with random motions[‡]. This could represent the scenario where the halo is formed by galactic satellites. Applying the virial theorem $M_{dyn} = \frac{5}{G} \frac{R V_v^2}{2}$ (Carroll & Ostlie 1999), where R is the radius of the system (40 kpc) and V_v is the radial velocity dispersion of the clouds within the halo (given by the σ of the emission lines $\sim 130 \text{ km s}^{-1}$) we obtain $M_{dyn} = 8 \times 10^{11} M_\odot$ (this is the total mass of the system, luminous+dark).

- Inflow: In this case $M_{inf} = \frac{R V_R^2}{2 G}$, where V_R is the infalling velocity of a particle at distance R from the central mass M_{inf} . We have assumed that the axis of the ionized cones (opening angle $\theta=90^\circ$) is on the plane of the sky. The emission at each spatial position along the slit results from the integration of the gas emission within the cone slice inside the slit and along the line of sight (see Fig. 8). In such case, the FWZI of the narrow emission line at a given slit position gives the maximum projected velocity displacement between the gas at the two opposite edges of the slice cone in that spatial position, i.e., $FWZI = V_{02} - V_{01} = 2 \times V_R \sin(\theta/2)$, where $V_{02} = -V_{01} = V_R \sin(\theta/2)$. On the other hand, $R = \frac{r}{\cos(\theta/2)}$, where r is the observed projected radius. Therefore

$$M_{inf} = \frac{r}{\cos(\theta/2)} \left(\frac{FWZI}{2 \sin(\theta/2)} \right)^2 \frac{1}{2 G} \quad (3)$$

In USS0828+193, $FWZI \sim 430 \text{ km s}^{-1}$ at $r = 40 \text{ kpc}$ (8 arcsec) as measured from the spectrum. We obtain $M_{inf} \sim 6 \times 10^{11} M_\odot$ for the total mass of the system.

Values of this order have been estimated for the masses of low redshift radio galaxies and are smaller than typical masses of cD elliptical galaxies at low redshift (Tadhunter, Fosbury & Quinn 1989). If this result is confirmed, we would conclude that USS0828+193 will not become like the cD galaxies we see at the present epoch, unless mergers are involved.

Is it possible that the material in the halo is falling towards the center in a cooling flow manner (rather than in free fall) ?[§] We have investigated whether this scenario is plausible. We have assumed that the emission line gas is in pressure equilibrium with the hot phase. Typical temperatures of $T_{clouds} = 10\,000 \text{ K}$ and $T_{hot} = 10^7$ for the optical emitting gas and the hot phase respectively and $n_{clouds} = 50 \text{ cm}^{-3}$ for the emission line gas (§4.2), give $n_{hot} = 0.05 \text{ cm}^{-3}$ (the uncertainties on n_{clouds} and T_{hot} allow only crude estimates in the discussion that follows).

Adopting a value for the cooling function $\gamma(T=10^7 \text{ K}) = 5 \times 10^{-23} \text{ erg cm}^3 \text{ s}^{-1}$ (Raymond, Cox & Smith 1976), and combining the three equations in §3 (Nulsen, Stuart & Fabian 1984) the mass of hot gas in the halo (inside the visible radius of 40 kpc) of USS0828+193 is $\sim 4 \times 10^8 M_\odot$ and its radiative cooling time is $\sim 6 \times 10^7$ years. This cooling time is rather short (much shorter than the age of the Universe at that time). On this basis, it is possible that the gas we observe from the LSBH has cooled from the hot phase.

[‡] Pettini et al. (2001) also calculate dynamical masses of Ly break galaxies in terms of gas clouds.

[§] In the free fall scenario, the only force acting on the gas is gravity. In the cooling flow scenario, the pressure gradient in a hot corona acts against gravity

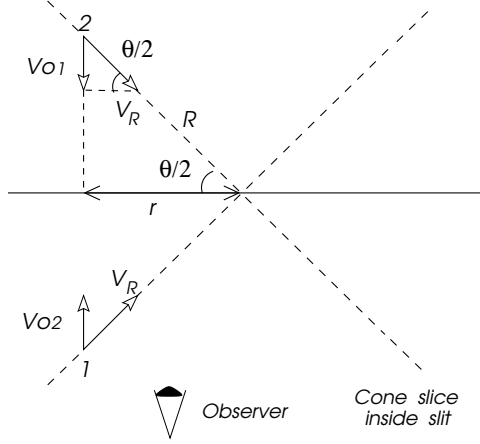
Calculating the total mass in the infalling scenario

Figure 8. Infall scenario: V_{o1} and V_{o2} are the velocities of particles in positions 1 and 2, projected on the line of sight (l.o.s) and V_R is the radial (infalling) velocity towards the center.

The mass that has cooled down is $\sim 10^9 M_\odot$ (considering only the ionized gas in the LSBH [see §4.2]). If this happened in $\sim 6 \times 10^7$ yr, the mass deposition rate is $17 M_\odot \text{ yr}^{-1}$ (values of this order have been measured in nearby cooling flow galaxies, Heckman, Armus & Miley 1990)

We have assumed that the density of the halo is constant. However, this is a very simplified scenario and the density profile is likely to be centrally condensed (Haiman and Rees 2001, HR2001 hereafter). The cooling time varies as n_e^{-1} (Nulsen, Stewart & Fabian 1984), therefore, the outer, less dense gas will need longer time to cool down. As van Ojik et al. found, when we account for this effect, the cooling time is still rather short at large distances ($r=100$ kpc) for a density behaviour of both $\propto r^{-1}$ and $\propto r^{-2}$ (2×10^8 and 2.5×10^8 years respectively). There has been, therefore, enough time for the gas to cool down.

In a cooling flow scenario, we expect very narrow emission lines at large distances ($\leq 100 \text{ km s}^{-1}$ at \geq tens kpcs, Fabian et al. 1987),[¶] a chaotic pattern in the velocity curve and a trend of the line width to decrease with increasing radius (Heckman et al. 1989). This behaviour is not obvious on the data but we are limited by the low spectral resolution. The kinematic properties of the halo do not help to constrain the validity of the cooling flow scenario. Higher resolution would help to measure the FWHM more accurately at different spatial position.

- Outflow: the halo could have been deposited by massi-

[¶] Emission lines as broad as several hundred km s^{-1} are observed in low redshift cooling flow nebulae (e.g. Fabian et al. 1987, Heckman et al. 1989). The authors propose that galaxy interactions may generate turbulence.

ve outflows (winds could explain the existence of heavy elements in the halo). We have calculated some basic parameters characterizing a superwind which could explain the kinematic properties of the LSBH in USS0828+193. The energy injection rate for an energy-conserving bubble inflated by energy injected at a constant rate and expanding into a uniform medium with an ambient density n_0 (cm^{-3}) is related to the radius (in kpc) and velocity (in 10^2 km s^{-1}) by (Heckman, Armus & Miley 1990)

$$dE/dt = 3 \times 10^{41} r_{\text{kpc}}^2 v_{100}^3 n_0 \text{ ergs}^{-1} \quad (4)$$

and the dynamical time scale of the nebula is given by

$$t_{\text{dyn},6} \sim 10 r_{\text{kpc}}/v_{100} \text{ Myr} \quad (5)$$

where v_{100} would be halve the separation in velocity between the two components of the double peaked profile produced by the expansion.

The resolution of the spectrum is too low to resolve the double peak that the expansion of the bubble would produce. We have estimated that two unresolved emission lines separated by a given velocity δv would produce a line of $\text{FWHM} \geq 2 \times \delta v = 4 \times v_{100}$ (all velocities in units of 100 km s^{-1}). Therefore, from the measurements in our spectrum ($\sigma \sim 130 \text{ km s}^{-1}$) we obtain $v_{100} \leq 0.76$.

The estimated density $n_e = 50 \text{ cm}^{-3}$ is probably the density of the post-shock gas in the expanding bubble. n_0 in the dE/dt equation is, however, the pre-shock density, which is likely to be much smaller (\sim several cm^{-3} , Heckman, Armus & Miley 1990). For $n_e = 1 \text{ cm}^{-3}$ the implied values of t_{dyn} and dE/dt are ~ 530 Myr (the corresponding time scale for ARP 220 is ~ 100 Myr, Heckman, Armus & Miley 1990) and $2.1 \times 10^{44} \text{ erg s}^{-1}$ respectively. The required star forming rate is $\text{SFR} \sim 500 M_\odot$ and a supernova rate of $\sim 4 \text{ SN yr}^{-1}$. Typical SFR values for Ly break galaxies (dust corrected) are several hundred $M_\odot \text{ yr}^{-1}$ (e.g. Sawicky & Yee 1998).

The expected total infrared luminosity of such a system would be $L_{\text{IR}} \sim 3 \times 10^{12} L_\odot$. This would place USS0828+193 in the category of ultraluminous infrared galaxies.

The kinematic signature of an expanding bubble (or bi-conical structure) would be a region of double peaked emission line profiles. Higher spectral resolution might reveal this pattern.

4.5 Is this a halo from which the galaxy is still forming ?

As Haiman & Rees discuss (2001), in the process of formation of a galaxy, smooth gas collapses from the virial radius to its final orbit radius. Numerical simulations have revealed a more complex process, where a fraction of the infalling gas forms smaller clumps early on; these clumps then progressively merge together, collide and dissipate to form larger systems. In these scenarios, a robust feature of galaxy formation is at least in the early stages a spatially extended distribution of gas. HR2001 showed that if the halo is illuminated by ionizing radiation from a central quasar, it should be observed as an extended $\text{Ly}\alpha$ fuzz with surface brightness $\sim 10^{-17} \text{ erg s}^{-1} \text{ cm}^{-2} \text{ arcsec}^{-2}$.

We compare in this section the properties of the LSBH in USS0828+193 with those expected for the extended gas condensation in the early stages of galaxy formation models.

• **Total mass:** At $z=3$ (total) halo masses in the range $\sim 4 \times 10^{10} - 10^{13} M_{\odot}$ are expected for a virial temperature in the range $T_{\text{vir}} = 2 \times 10^5 \text{ K} - 2 \times 10^7 \text{ K}$ (HR2001). We have obtained $M_{\text{tot}} \sim 6 - 8 \times 10^{11} M_{\odot}$ for the two scenarios (infall and virialized system of clouds) where we have been able to calculate the total mass of the system. This value lies in the range predicted by the models.

• **F(Ly α)_{SB}:** The expected surface brightness for the Ly α fuzz is in the range $\sim 10^{-18} - 10^{-16} \text{ erg s}^{-1} \text{ cm}^{-2} \text{ arcsec}^{-2}$ (HR2001). This is consistent with the measured value in USS0828+193 $\sim 3 \times 10^{-17} \text{ erg s}^{-1} \text{ cm}^{-2} \text{ arcsec}^{-2}$.

• **Linear size:** The linear spatial extension of the Ly α emitting gas would be a fraction of the virial radius $R_{\text{vir}} \sim 10 - 100 \text{ kpc}$ (HR2001), consistent with the linear scale of the halo (radius) in USS0828+193, $\sim 40 \text{ kpc}$.

• **Black hole mass:** According to HR2001 model, the minimum mass required to ionize the halo is given by:

$$M_{\text{bh}} \sim 6 \times 10^8 M_{\odot} \left(\frac{M_{\text{tot}}}{10^{12} M_{\odot}} \right)^{5/3} \left(\frac{1+z}{6} \right)^4 \quad (6)$$

Assuming $M_{\text{tot}} = 8 \times 10^{11} M_{\odot}$ as above, we find a lower limit for the black hole mass of $\sim 5 \times 10^7 M_{\odot}$. This value is somewhat lower than the black hole mass we expect according to Gu, Cao and Jiang (2001), who found that the vast majority of the quasars in the 1Jy, S4 and S5 catalogues have typical black hole masses of $\geq 10^8 M_{\odot}$.

• **Heavy elements:** One of our most important results is the finding of heavy elements in the LSBH. Any model of protogalactic halos should consider metal enrichment. This is mentioned by HR2001, although not discussed in details.

The properties of the low surface brightness halo in USS0828+193 are, therefore, consistent with the expected properties for the extended gaseous halo, a required ingredient for galaxy formation models.

However, the existence of the halo does not necessarily imply that USS0828+193 is a galaxy in the process of formation. Similar halos have been found in lower redshift radio galaxies, where the galaxy is expected to be fully formed. An example is the radio galaxy 3C368 at $z=1$ (Stockton, Ridgway & Kellogg 1996). This object shows low surface brightness [OII] 3727 emission with apparently quiescent kinematics, in addition to the bright kinematically perturbed structures. Other examples at lower redshift are 3C34 ($z=0.69$), 3C435A ($z=0.47$) (see 2-dimensional [OII] 3727 spectra in Solórzano-Iñarra, Tadhunter & Axon (2001)). The halos extend for more than 100 kpc). Such halos might be similar to the LSBH we have discovered in the Ly α light in our more distant radio galaxies. If this is the case, the existence of LSBH associated with distant radio galaxies does not imply an early stage in the formation process. On the other hand, the consistency of the LSBH properties in USS0828+193 with expectations for the initial gas reservoir, suggests that the halo gas is part of the material from which the galaxy started to grow.

4.5.1 Comparison with other objects

We discuss here several structures found around other types of galaxies at different redshifts which might have the same origin as the low surface brightness halos found around distant radio galaxies.

• **Galactic envelopes:** observations of absorption line systems in the spectra of background quasars have provided evidence for large ($R \sim 100 h^{-1} \text{ kpc}$) extended gaseous envelopes that surround galaxies of a wide range of luminosity and morphological type (e.g. Chen, Lanzetta & Webb 2001; Lanzetta et al. 1995). Chen, Lanzetta & Webb (2001) have proposed accreting satellites as the origin of these structures to explain the chemical enrichment at large distances.

• **Giant Ly α halos associated with Ly break galaxies:** Steidel et al. (2000) found two giant (physical extent $\geq 100 h^{-1}$) diffuse Ly α emitters apparently associated with previously known Ly break galaxies at $z \sim 3.09$. The origin of these structures is not clear. Proposed explanations are a cooling flow nebula (Steidel et al. 2000) or 'hyperwinds' (Taniguchi, Shioya & Kakazu, 2001).

• **Large scale (\geq several tens of kpc) HI disc like structures** have been found in several low redshift radio (Morganti et al. 2002) and elliptical galaxies (Oosterloo et al. 2002). The authors propose that these structures are the results of mergers. The LSBH found around USS 0828+193 and other distant radio galaxies, might be the progenitors of the discs found at low redshift.

Therefore, giant gaseous halos (\geq several tens of kpc) are found to be often associated with galaxies in general: active and non active, of different morphological types and luminosities and at different epochs. The origin and nature of such halos is not clear and different explanations have been proposed for different objects, but the definitive answer is uncertain. An interesting possibility is that these halos have a similar origin related to the formation process of the galaxies.

5 SUMMARY AND CONCLUSIONS

By means of the spectral decomposition of the emission line profiles in USS0828+193, we have isolated the emission from a giant ($\sim 80 \text{ kpc}$) reservoir of apparently kinematically unperturbed gas, whose kinematics is consistent with being gravitational in nature. Emission lines other than Ly α (CIV, HeII) have been detected for the first time in such a halo. This implies that the gas is ionized (probably by the continuum from the AGN) and enriched with heavy elements. We find marginal evidence for continuum detection from the halo.

We propose that the low surface brightness halo in USS0828+193 (and other HzRG) could be part of a gaseous reservoir that surrounds the entire object. We have considered several possible scenarios to explain the origin of the halo. The gas could have settled in a rotating disc. This is suggested by the velocity pattern of the halo emission, although 3-dimensional spectroscopy would be necessary to set tighter constraints on the kinematic patterns. Evidence for giant gaseous discs has been found by other authors in low redshift radio galaxies and elliptical galaxies.

The halo could also be a group of individual clouds (galactic satellites?) in a virialized system. In this case, the expected mass is $\sim 8 \times 10^{11} M_{\odot}$. A similar value is estimated if the halo is infalling towards the center of the potential well. Such values are similar to estimates of masses of low redshift radio galaxies, and smaller than typical masses of

cD elliptical galaxies at low redshift. If this result is confirmed, we conclude that USS0828+193 will not become like the cD galaxies we see at the present epoch, unless mergers are involved.

Alternative scenarios that we have discussed (also consistent with the observations) are a cooling flow from a hot phase and outflows (galactic winds). In this last case, star forming rates $\sim 500 M_{\odot} \text{ yr}^{-1}$ are required, consistent with estimates for Lyman break galaxies.

The properties of the low surface brightness Ly α halo detected in the radio galaxy USS0828+193 are consistent with the expectations for the original gaseous reservoir from which the galaxy started to form. This does not necessarily imply that the galaxy is in the process of formation.

We have also discussed the possible link of the low surface brightness halos with a) the very extended envelopes found around galaxies of different morphological types and luminosities based on studies of absorption line systems in the spectra of background quasars b) the giant Ly α halos associated with some Ly break galaxies c) the very extended reservoirs (claimed to be discs) of neutral gas associated with some nearby radio galaxies and elliptical galaxies.

ACKNOWLEDGMENTS

MVM thanks Jochen Liske for useful discussion on quasar absorption line systems and galactic envelopes.

REFERENCES

- Barthel P., 1989, *ApJ*, 336, 606
 Baum S., Heckman T., van Breugel W., 1990, *ApJS*, 74, 389
 Baum S., McCarthy P., 2000, *AJ*, 119, 2634
 Binette L., Kurk J., Villar-Martín M., Röttgering H., 2000, *A&A*, 356, 23
 Böhringer H., 1985, *RvMA*, 8, 2595
 Carilli C., Röttgering H., van Ojik R., Miley G., van Breugel W., 1997, *ApJS*, 109, 1
 Carroll B., Ostlie D., 1999, in *An Introduction to Modern Astrophysics*. Addison-Wesley Publishing Company
 Chambers K., Miley G., van Breugel W., 1990, *ApJ*, 363, 21
 Chen H.-W., Lanzetta K., Webb J., 2001, *ApJ*, 556, 158
 Clark N., Axon D., Tadhunter C., Robinson C., O'Brien P., 1998, *ApJ*, 494, 546
 Fabian A., Crawford C., Johnstone R., Thomas P., 1987, *MNRAS*, 963
 Goodrich R., Cohen M., Putney A., 1995, *PASP*, 107, 179
 Gu M., Cao X., Jiang D., 2001, *MNRAS*, 327, 1111
 Haiman Z., Ress M., 2001, *ApJ*, 556, 87 (HR2001)
 Heckman T., Illingworth G., Miley G., van Breugel W., 1985, *ApJ*, 299, 41
 Heckman T., Baum S., van Breugel W., McCarthy P., 1989, *ApJ*, 338, 48
 Heckman T., Armus L., Miley G., 1990, *ApJS*, 74, 833
 Heckman T., Lehnert M., van Breugel W., Miley G., 1991, *ApJ*, 370, 78
 Kurk J., Röttgering H., Miley G., Pentericci L., 2001, *astro-ph/0102337*
 Lanzetta K., Bowen D., Tytler D., Webb J., 1995, *ApJ*, 442, 538
 Lehnert M., Becker R., 1998, *A&A*, 332, 514
 McCarthy P.J., Spinrad H., van Breugel W., Liebert J., Dickinson M., Djorgovski S., Eisenhardt P., 1990a, *ApJ*, 365, 487
 McCarthy P., Spinrad H., Dickinson M., van Breugel W., Liebert J., Djorgovski S., Eisenhardt P., 1990b, *ApJ*, 365, 487
 McCarthy P.J., Baum S., Spinrad H., 1996, *ApJS*, 106, 281
 Morganti R., Oosterloo S., Tinti S., Tadhunter C., Wills K., van Moorsel G., 2002, *astro-ph/0112269*
 Nulsen P., Stuart G.C., Fabian A., 1984, *MNRAS*, 208, 185
 Oke et al., 1995, *PASP*, 107, 375
 Oosterloo T., Morganti R., Sadler E., Vergani D., Caldwell N., 2002, *AJ*, 123, 729
 Pettini M., Shapley A., Steidel C., Cuby J.C., Dickinson M., Moorwood A., Adelberger K., Giallisco M., 2001, *ApJ*, 554, 981
 Pentericci L., McCarthy P., Röttgering H., Miley G., McCarthy P., Spinrad H., van Breugel W., Macchetto F., 1999, *A&A*, 341, 329
 Raymond J., Cox D., Smith B., 1976, *ApJ*, 204, 290
 Röttgering H., Miley G., Chambers K.C., 1995, *A&AS*, 114, 51
 Röttgering H., Hunstead R., Miley G., van Ojik R., Wieringa M., 1995, *MNRAS*, 277, 389
 Sawicky & Yee, 1998, *AJ*, 115, 1329
 Steidel C., Adelberger K., Shapley A., Pettini M., Dickinson M., Giallisco M., 2000, *ApJ*, 532, 170
 Solórzano-Iñarra C., Tadhunter C., Axon D., 2001, *MNRAS*, 323, 965
 Stockton A., Ridgway S., Kellogg M., 1996, *AJ*, 112, 902
 Tadhunter C., Fosbury R., Quinn P., 1989, *MNRAS*, 240, 225
 Taniguchi Y., Shioya Y., Kakazu Y., 2001, *ApJ*, 562, 15
 Thomas P., 1988, *MNRAS*, 235, 315
 van Ojik R., Röttgering H., Carilli C.L., Miley G.K., Bremer M.N., Macchetto F., 1996, *A&A*, 313, 25
 van Ojik R., Röttgering H., Miley G., Hunstead R., 1997, *A&A*, 317, 358
 Vernet J., Fosbury R., Villar-Martín M., Cohen M., Cimatti, A.; di Serego Alighieri S., Goodrich R., 2001, *A&A*, 366, 7
 Villar-Martín M., Binette L., Fosbury R., 1996, *A&A*, 312, 751
 Villar-Martín M., Tadhunter C., Clark N., 1997, *A&A*, 323, 21
 Villar-Martín M., Binette L., Fosbury R., 1999, *A&A*, 346, 7
 Villar-Martín M., Alonso-Herrero A., di Serego-Alighieri S., Vernet J., 2001, *A&A*, 147, 291